Journal of Applied Polymer Science

Synthesis and mechanical properties of high impact polystyrene with *in situ* bulk polymerization toughened by one-pot Nd-based styrene–isoprene–butadiene terpolymer rubber

Tingting Li, Li Li, Qiang Xu, Yurong Wang, Yang Li

State Key Laboratory of Fine Chemicals, Department of Polymer Science and Engineering, Dalian University of Technology, Dalian, Liaoning, 116024, China

T. Li and L. Li contributed equally to this work.

Correspondence to: Y. Li (E-mail: liyang@dlut.edu.cn)

ABSTRACT: High impact polystyrene (HIPS) resins were obtained with *in situ* bulk polymerization toughened by styrene–isoprene–butadiene terpolymer rubber (SIBR). SIBR prepolymer was prepared through selective polymerization of styrene (St), isoprene (Ip), and butadiene (Bd) in St with [Nd]/[Al]/[Cl] catalyst. Nd-based catalyst exhibited more favorable activity toward conjugated diene other than St, resulting in St solution of random SIBR with high *cis*-1,4 stereoregularity and low St content, which was directly exposed to the free radical polymerization of St to generate HIPS. Effect of toughened rubber and the initiators [difunctional (D2) and trifunctional (T3)] were examined to attain HIPS possessing mechanical properties as follow: impact strength, 0.9–24.8 kJ/m^2; tensile strength, 16.0–27.5 MPa; and elongation at break, 7.4–107.0%. Increasing SIBR matrix in HIPS improved the impact strength and decreased tensile strength. The fracture surface morphologies of HIPS specimens were studied by notched impact tests and scanning electron microscopy (SEM), illustrating that the incremental SIBR matrix presented synergistic toughening effect of crazing to enhance the ductile fracture behavior. © 2016 Wiley Periodicals, Inc. J. Appl. Polym. Sci. **2016**, *133*, 43979.

KEYWORDS: HIPS resins; *in situ* bulk polymerization; mechanical properties; Nd-based catalyst; SIBR

Received 17 February 2016; accepted 25 May 2016

DOI: 10.1002/app.43979

INTRODUCTION

High impact polystyrene (HIPS) resin is an important elastomer-toughened thermoplastic that provides an excellent balance between rigidity and elasticity, which is superior to general purpose polystyrene (PS).[1,2] In the bulk HIPS process, the radical polymerization of styrene (St) is carried out in the presence of dissolved polybutadiene (PB),[3,4] resulting in PB rubber matrix grafted with PS sequences to provide high impact toughness. In the beginning of the heterogeneous polymerization period, the disperse phase is mainly PS while the continuous phase is referred to the rubber matrix. Along with the conversion increases, a phase inversion period occurs and the graft copolymer accumulates in favor of forming the "salami" or "core-shell" morphology.[3,4] In view of polymerization process simplification and economic efficiency, the procedure is substituted by "in situ" bulk polymerization. The polymerization of butadiene (Bd) occurs in St solvent to provide a rubber solution, then the added initiator induces radical polymerization of unreacted St.[5–10] The selective catalysts toward Bd monomer in St solvent is focused on alkyl lithium,[5,6] transition metal catalyst,[7,8] and rare earth metal catalyst.[9,10] Comparing with alkyl lithium, transition metal catalyst shows better selective activity and higher regio/stereoselectivity without formation of PS block sequences. However, the remove process of transition metal catalyst is essential to avoid facile aging caused by varied valence state. Nd-based rare earth catalyst turns out to be an optimal choice, owing to the high *cis*-1,4 regularity, selective activity and constant 3+ valence state.[11–15] The rubber matrix with high *cis*-1,4 regularity offers HIPS resin to perform high impact strength even at low temperature and much higher energy to cause failure.[16]

Based on the investigation of HIPS toughened by PB, St–Bd copolymer rubber (SBR) is utilized as a superior rubber matrix.[17–21] St units in random SBR rubber are proven to enhance its compatibility with PS matrix, without sacrifice of toughening effect.[19,20] Styrene–isoprene–butadiene terpolymer rubber (SIBR) was reported by Nordsiek in 1984.[22] Because of the outstanding balance of low rolling resistance, skid resistance, and abrasion resistance, it is considered as an excellent integral rubber. When PB is substituted by SIBR as rubber matrix, St-based resins [HIPS/Acrylonitrile-Butadiene-Styrene Plastic Copolymer (ABS)] exhibit higher impact strength with regular "stereo-network" morphology.[23–25] However, SIBR served as toughened rubber for HIPS is mainly obtained via anionic polymerization, which possesses low *cis*-1,4 content. It is

Table I. Polymerization of St/Ip/Bd with Nd-Based Catalyst[a]

Prepolymer	St/Ip/Bd (mol %)	$M_w \times 10^{-4}$	M_w/M_n	S/I/B (wt %)	PB (mol %)		PI (mol %)	
					1,4-	1,2-	1,4-	3,4-
SIBR-1[b]	5/1/1	44.9	4.2	3/48/49	98	2	97	3
SIBR-2[c]	5/1/1	19.8	4.3	10/42/48	97	3	96	4
SIBR-3[d]	10/1/1	17.2	4.8	24/36/40	98	2	96	4

[a] Condition: [Nd]/[Al]/[Cl] molar ratio was 1:15:3, M_w and M_w/M_n were determined by GPC, polymer components and microstructure were examined by NMR.
[b] $Nd(P_{204})_3/Al^iBu_2H/^tBuCl$, $[Nd]/[Bd + Ip] = 6 \times 10^{-6}$ mol/g.
[c] $Nd(P_{204})_3/Al^iBu_2H/CHCl_3$, $[Nd]/[Bd + Ip] = 6 \times 10^{-6}$ mol/g.
[d] $Nd(P_{204})_3/Al^iBu_2H/CHCl_3$, $[Nd]/[Bd + Ip] = 8 \times 10^{-6}$ mol/g.

well-known that rubbers with high *cis*-1,4 content possess excellent elasticity, which can further improve the toughness effect. SIBR initiated by Nd-based rare earth catalyst is reported recently, which shows high *cis*-1,4 selectivity and random distribution.[18,26] To the best of our knowledge, the novel Nd-based SIBR served as toughened rubber to prepare in situ HIPS resins has not been probed.

HIPS resins play an important role in the engineering field, so the strategy to produce high-performance HIPS remains an attractive issue in both of academic research and industrial application.[27–32] Herein, the terpolymerization of St, isoprene (Ip) and Bd by Nd-based catalyst was implemented in St solvent, affording St solvent of SIBR rubber matrix in situ. Then, the rubber solution was directly subject to the multi-functional initiator to carry out radical polymerization, resulting in HIPS resin toughened by random SIBR with high *cis*-1,4 selectivity. The effects of SIBR type, rubber content, and initiator type on the microstructure, macromolecular weight (M_w), and relative mechanical properties of HIPS were illustrated. The toughening mechanism was investigated by examining the morphology of impact fracture surface.

Table II. Synthesis of HIPS with *In Situ* Bulk Polymerization[a]

Sample no.	Prepolymer	Initiator	Initiator (wt %)	Rubber (wt %)	RPVF (%)	GD (%)	PS		Impact strength (kJ/m^2)
							$M_w \times 10^{-4}$	M_w/M_n	
HIPS-1	SIBR-1	T3	0.02	5	5.2	5.0	20.3	2.4	1.8
HIPS-2	SIBR-1	T3	0.02	10	11.4	10.4	21.2	2.3	2.1
HIPS-3	SIBR-1	T3	0.02	15	24.6	39.5	22.3	2.6	2.5
HIPS-4	SIBR-1	T3	0.02	20	30.1	50.2	25.3	2.8	4.0
HIPS-5[b]	SIBR-2	D2	0.1	10	21.3	51.3	34.0	2.8	5.3
HIPS-6[b]	SIBR-2	D2	0.1	15	35.4	62.5	28.6	2.8	6.5
HIPS-7[b]	SIBR-2	D2	0.1	20	40.2	79.3	25.3	3.0	12.9
HIPS-8[b]	SIBR-2	D2	0.1	25	48.6	91.2	22.0	2.9	16.4
HIPS-9[b]	SIBR-2	D2	0.1	29	50.8	97.5	19.1	3.2	22.2
HIPS-10	SIBR-2	T3	0.02	5	5.1	9.2	25.2	2.8	1.7
HIPS-11	SIBR-2	T3	0.02	10	11.6	10.2	24.2	2.7	3.3
HIPS-12	SIBR-2	T3	0.02	15	25.3	43.6	23.8	2.5	7.2
HIPS-13	SIBR-2	T3	0.02	20	36.4	81.9	22.2	2.9	11.3
HIPS-14	SIBR-2	T3	0.02	25	43.1	86.4	21.8	2.9	14.3
HIPS-15	SIBR-2	T3	0.02	29	52.4	90.3	18.1	3.2	24.8
HIPS-16	SIBR-2	T3	0.01	20	30.2	70.1	24.2	2.7	15.6
HIPS-17	SIBR-2	T3	0.04	20	37.4	84.2	22.0	2.8	7.1
HIPS-18	SIBR-2	T3	0.10	20	37.0	83.5	19.0	2.9	6.5
HIPS-19	SIBR-3	T3	0.02	5	5.5	6.7	18.9	2.5	0.9
HIPS-20	SIBR-3	T3	0.02	10	11.5	10.5	19.2	2.6	1.0
HIPS-21	SIBR-3	T3	0.02	15	21.9	22.0	22.1	2.3	3.1
HIPS-22	SIBR-3	T3	0.02	20	29.2	43.9	21.8	2.4	3.9

[a] Initial temperature was 135 °C for 2 h; then the heating rate was 10 °C/h for 7 h; ethylbenzene content was 10 wt %.
[b] Initial temperature was 106 °C for 2 h; then the heating rate was 10 °C/h for 7 h; ethylbenzene content was 10 wt %.

EXPERIMENTAL

Materials

Neodymium bis(2-ethylhexyl) phosphate [$Nd(P_{204})_3$] was synthesized according to the reported method.[26] $CHCl_3$ was refluxed over CaH_2 for 2 h under nitrogen before distillation, then it is used as a hexane solution (1.0 *M*). Bd (North Huajin Chemical Industries Group Co., Liaoning, China) was treated with *n*-butyllithium to remove the moisture and inhibitor, and then vaporized to keep water content below 10 ppm. Ip and St (North Huajin Chemical Industries Group Co., Liaoning, China) was refluxed over CaH_2 for 2 h before distillation under nitrogen. Al^iBu_2H (1.0 *M* solution in hexane, Alfa-Aesear Co., Shanghai, China), a difunctional initiator (D2) [DP275B, 1,1-di-(*tert*-butylperoxy)-3,3,5-trimethylcyclohexane, North Huajin Chemical Industries Group Co., Liaoning, China], a trifunctional initiator (T3) (TETMTPA, 3,6,9-triethyl-3,6,9-trimethyl-1,4,7-triperoxonane, J&K Co., Beijing, China), and

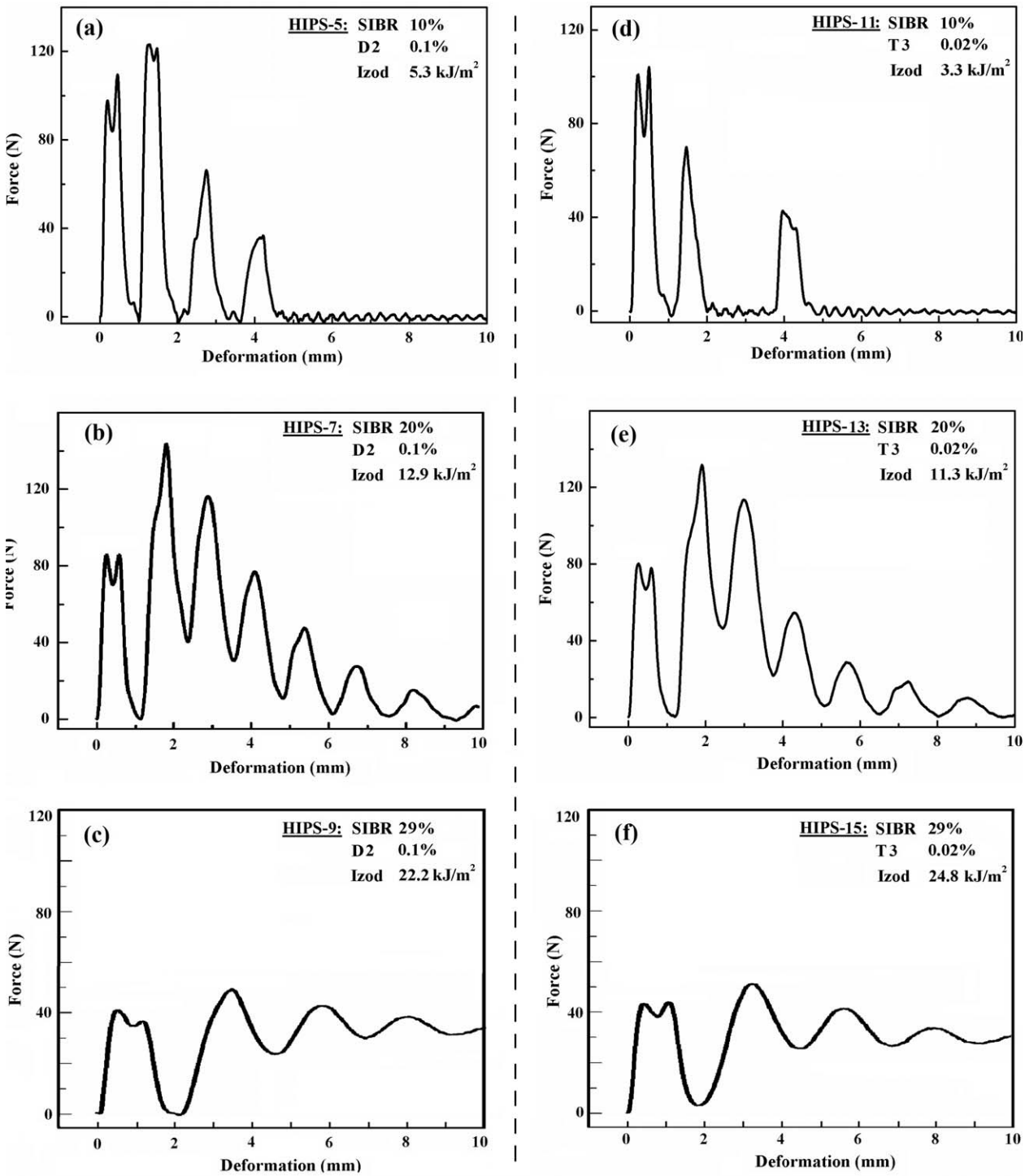

Figure 1. Impact curves of HIPS with different SIBR rubber content.

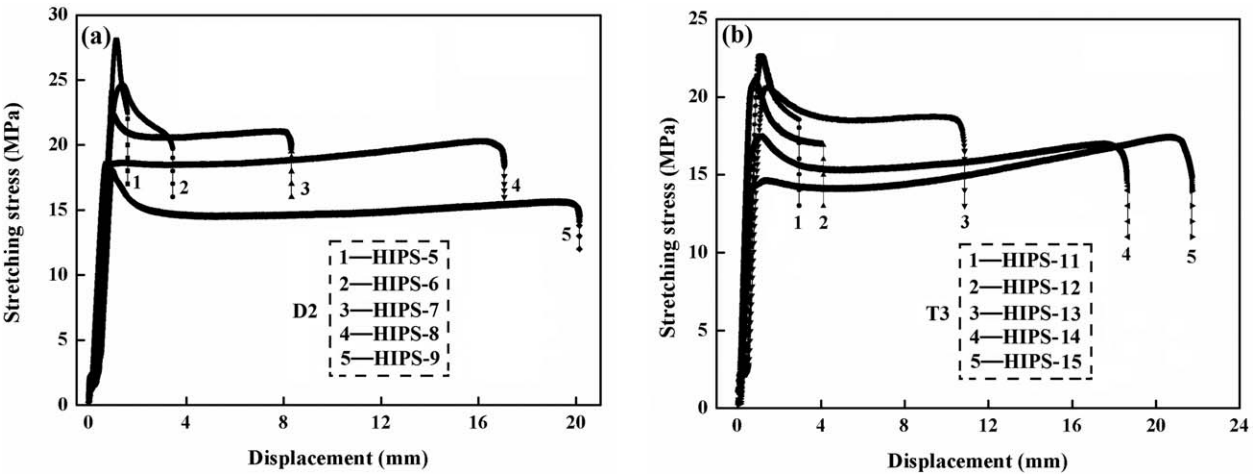

Figure 2. Tensile curves of HIPS with different SIBR rubber content.

ethylbenzene (Alfa-Aesear Co., Shanghai, China) were used as purchased.

In Situ Bulk Polymerization of HIPS Resin

All synthesis and polymerization were implemented under dry and inert atmosphere (N_2) via standard Schlenk techniques. A typical polymerization procedure was carried out connected to the Schlenk line and equipped with a rubber septum with nitrogen inlet. The ampoule tubes and flasks were treated with three cycles of flaming/nitrogen-purging/evacuating.

***In Situ* St Solution of SIBR Rubber Matrix.** $Nd(P_{204})_3$ (1 equiv.) and Al^iBu_2H (15 equiv.) were added into the reaction vessel with Ip (10 equiv.) as premonomer. After 10 min at room temperature, the mixture was observed as homogeneous solution. Then $CHCl_3$ or ^tBuCl ([Cl]/[Nd] = 3) was added, aging at 50 °C for 3 h.

St, Ip, and Bd were sealed in dry and N_2 atmosphere. Then a certain amount of preformed catalyst was injected. The polymerization lasted for 6 h at 50 °C. For analysis purpose, a small quantity of St solution of SIBR was drawn out by syringe and quenched by the acidified isopropanol containing 2,6-di-*tert*-butyl-4-methylphenol (1 wt %) as the stabilizer.

Table III. Effect of Rubber Content on Tensile Properties of HIPS

Sample no.	Initiator	Rubber (wt %)	Tensile strength (MPa)	Elongation at break (%)
HIPS-5	D2	10	27.5	7.4
HIPS-6	D2	15	24.6	16.9
HIPS-7	D2	20	22.5	41.1
HIPS-8	D2	25	20.4	83.6
HIPS-9	D2	29	18.1	100.6
HIPS-11	T3	10	23.2	14.3
HIPS-12	T3	15	21.1	19.6
HIPS-13	T3	20	20.6	53.1
HIPS-14	T3	25	17.5	92.0
HIPS-15	T3	29	16.0	107.0

Preparation of HIPS Resins. Ethylbenzene was added into St solution of SIBR prepared as the diluter. St was added according to the required rubber content in HIPS resins. The initiator was introduced to carry out in situ radical polymerization. When D2 was used as initiator, the initial polymerization condition was 106 °C for 2 h and then the mixture was continued to be heated with the rate of 10 °C/h for 7 h. When T3 was used as initiator, the initial polymerization condition was 135 °C for 2 h and then the mixture was continued to be heated with the rate of 10 °C/h for 7 h.

Characterization of SIBR

M_w and M_w/M_n of SIBR was measured by Gel Permeation Chromatograph (GPC) by a Waters 1515-2414 instrument, with PS as calibration and THF as eluent at 30 °C. The microstructure of SIBR was detected by ^1H NMR and ^{13}C NMR spectroscopy with Bruker spectrometer in $CDCl_3$ at room temperature, with the tetramethylsilane as an internal reference. The microstructure was also proven by Fourier transform infrared spectroscopy (FTIR) with Nicolet FTIR spectrophotometer with films on KBr discs.

Characterization of HIPS

Analysis of Grafting Parameters. HIPS (M_{HIPS}:0.150 g) was dissolved in mixed solution (30 mL) of acetone and methyl ethyl ketone (MEK) mixed solvent. After refluxed for 8 h, the solution was centrifuged at 8,000 r/min for 1 h. PS was precipitated through pouring the supernatant into a large amount of ethanol with intensive stirring. The insoluble portion was SIBR grafted with PS (SIBR-*g*-PS), which was repeatedly washed with acetone/MEK. Both of the two products were collected and dried under vacuum at 40 °C for 72 h. The constant weight of PS and SIBR-*g*-PS is M_{PS} and $M_{SIBR\text{-}g\text{-}PS}$. The weight of SIBR ($M_{SIBR}$) was calculated based on the obtained result above. The rubber phase volume fraction (RPVF) represents the weight fraction of SIBR-*g*-PS in HIPS resins, as shown in eq. (1). Grafting degree (GD) represents the weight fraction of PS in SIBR-*g*-PS toward SIBR, as demonstrated in eq. (2).[33–35]

$$\mathrm{RPVF} = \frac{M_{SIBR-g-PS}}{M_{HIPS}} \quad (1)$$

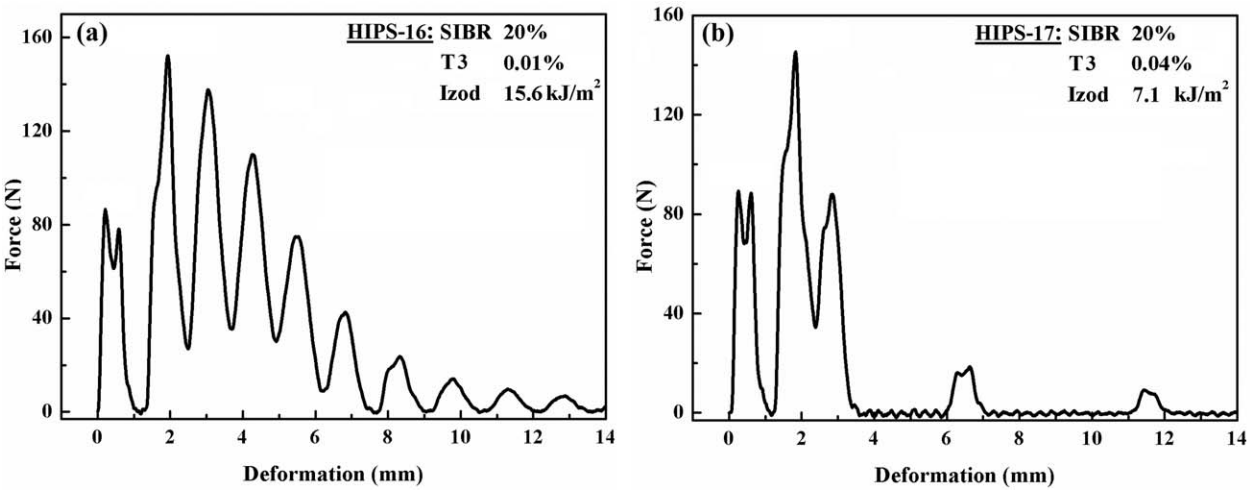

Figure 3. Impact curves of HIPS with different initiator content.

$$GD = \frac{M_{SIBR-g-PS} - M_{SIBR}}{M_{SIBR}} \quad (2)$$

Notched Impact Test and Tensile Test. The notched impact strength and impact curves were measured by a pendulum impact tester (CEAST 9050) equipped with 5.5 J hammer at 23 °C. The notched specimens were prepared with dimension of 80 mm × 10 mm × 4 mm and 2 mm depth V-notch by injection test sample molding apparatus (RAY-RAN RR3400) according to ISO 180:2000 standard. The corresponding tensile property was examined using INSTRON 5567 Universal Tensile Tester according to ISO 527-1:1993 standard at 23 °C with crosshead speed of 5 mm/min.

Morphology of Impact Fracture Surface. The morphology of impact fracture surfaces were observed by FEI QUANTA200 SEM with a working voltage of 20 kV in order to analyze the fracture nature and deformation mechanism, and the specimens were coated with a thin gold layer on a K550X Sputtering Coater (EMITECH) before observation.

RESULTS AND DISCUSSION

Polymerization of St, Ip, and Bd in St

Random SIBR were obtained in St with Nd-based catalyst, as shown in Table I. In the ^{1}H NMR spectrum, there were signals located at 6.85–7.40 ppm with absence of 6.20–6.85 ppm, which assigned to the random and block St sequences, respectively. This illustrated that SIBR obtained with Nd-based catalyst possessed random distribution.[36] Peaks appeared around 5.38 and 4.95 ppm were assigned to 1,4-Bd and 1,2-Bd units, while signals of 1,4-Ip and 3,4-Ip units could be observed around 5.12 and 4.70 ppm.[37,38] Peaks around 23.7, 16.3, and 18.9 ppm in ^{13}C NMR spectrum were assigned to *cis*-1,4, *trans*-1,4, and 3,4-Ip units. IR spectrum showed intensive signals around 734 cm^{-1} which assigned for *cis* 1,4-PB structure.[39] According to nuclear magnetic resonance (NMR) and infrared (IR) analysis, SIBR possessed high 1,4 content of Bd units and Ip units. By tuning the catalyst system and feed ratio, random SIBR with different contents of St groups (3–24 wt %) were generated.

Table IV. Effect of Initiator Content on the Tensile Property of HIPS

Sample no.	Initiator	Initiator (wt %)	Tensile strength (MPa)	Elongation at break (%)
HIPS-16	T3	0.01	23.2	66.2
HIPS-13	T3	0.02	20.6	53.1
HIPS-17	T3	0.04	20.0	46.5
HIPS-18	T3	0.10	19.9	42.6

Synthesis and Mechanical Properties of HIPS Resins

HIPS resins were prepared by the *in situ* bulk polymerization of styrene in the presence of one-pot St solution of SIBR rubber matrix. Herein, three types of SIBR prepolymer were examined to toughen PS with T3 as initiator in the radical polymerization. St units content of SIBR-1, SIBR-2, and SIBR-3 were 3, 10, and 24 wt %, respectively (Table I).As shown in Table II, HIPS-1–HIPS-4 were toughened by SIBR-1 with the rubber matrix fraction increased from 5 wt % to 20 wt %, resulting in increased RPVF (5.2–30.1%), GD (5.0–50.2%), and impact strength (1.8–4.0 kJ/m^2). When SIBR-2 was selected as the prepolymer to produce HIPS-10–HIPS-13 (SIBR content: 5–20%), HIPS resins exhibited higher RPVF (5.1–36.4%), GD (9.2–81.9%), and impact strength

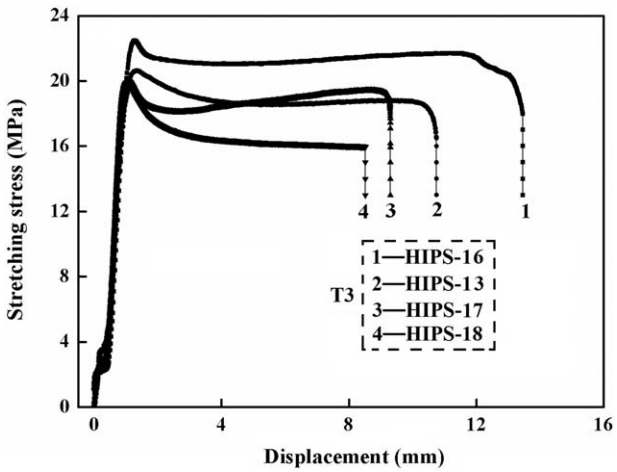

Figure 4. Tensile curves of HIPS with different initiator content.

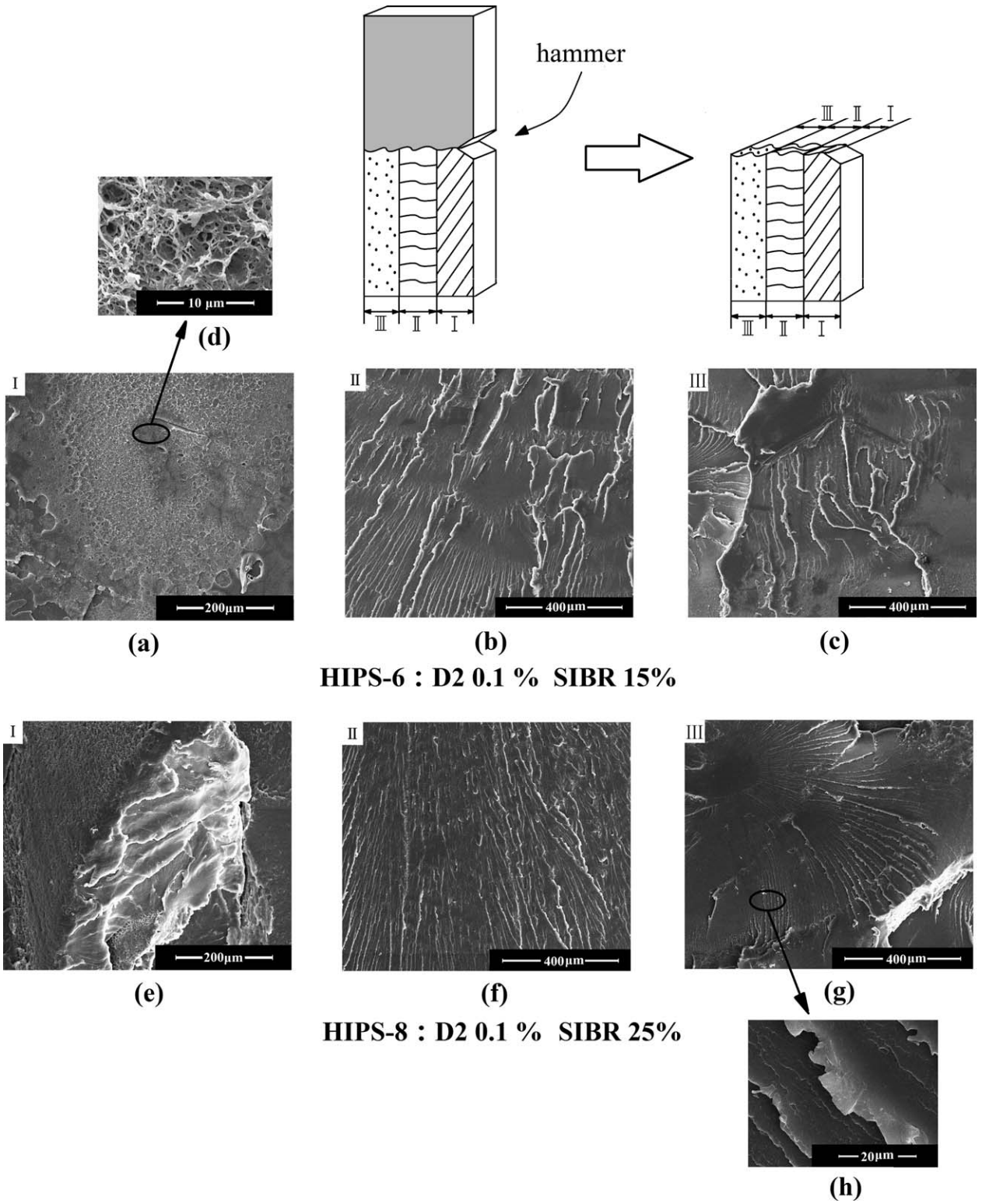

Figure 5. SEM micrographs of HIPS.

(1.7–11.3 kJ/m^2). Consequently, the impact strength was significantly enhanced with the better compatibility between rubbery and plastic phase caused by the increased St content in SIBR. When HIPS resins were toughened by SIBR-3 (5–20 wt %), HIPS-19–HIPS-22 possessed lower RPVF (5.5–29.2%), GD (6.7–43.9%), and impact strength (0.9–3.9 kJ/m^2) parameters. This diminished toughening effect was on the account of the reductive rubber elasticity along with the further increased St content. As a result, SIBR-2 was confirmed as a superior rubber matrix to toughen HIPS resins. As for all the SIBR prepolymers, the increased rubber matrix

fraction obviously resulted in raised RPVF, GD, and impact strength.

As described in Table II, HIPS-5–HIPS-9 were obtained by difunctional initiator (D2) toughened by SIBR-2. RPVF (21.3–50.8%) and GD (51.3–97.5%) were obviously enhanced with incremental SIBR weight fraction of 10–29%. In this process, the impact curves tend to exhibit continuous characteristic in the impact curves. HIPS-5–HIPS-9 showed improved impact strength from 5.3 to 22.2 kJ/m^2 [Figure 1(a–c)] and decreased tensile strength from 27.5 to 18.1 MPa, while elongation at break expanded from 7.4% to 100.6%. Figure 2(a) exhibited obviously increased displacement at break from HIPS-5 to HIPS-9 with sequentially incremental SIBR content (10–29 wt %).

Trifunctional initiator T3 was also examined to produce sample HIPS-11–HIPS-15 in Table II. When SIBR-2 fraction increased from 10% to 29%, the incremental range of RPVF and GD was 11.6%–52.4% and 10.2%–90.3%, respectively. Meanwhile, the impact strength apparently enhanced from 3.3 to 24.8 kJ/m^2 (Table II), with impact curves tended to present continuous feature as shown in Figure 1(d–f). In this procedure, the tensile strength depressed from 23.2 to 16.0 MPa (Table III), while the elongation at break increased from 14.3% to 107.0% with displacement at break raised from 2.9 to 21.7 mm as illustrated in Figure 2(b).

The effect of initiator concentration on HIPS resins was also examined as shown in Table II. When SIBR weight fraction was fixed at 20%, initiator T3 concentration of 0.01–0.10 wt % were investigated, resulting in HIPS-16, HIPS-13, HIPS-17, and HIPS-18. Raising T3 concentration, RPVF (30.2–37.4%), and GD (70.1–84.2%) improved insignificantly while M_w of PS matrix decreased from 24.2 $\times$ 10^4 to 19.0 $\times$10^4. The increased content of T3 caused the impact strength declined obviously (15.6–6.5 kJ/m^2), as shown in Figure 3. Tensile strength (23.2–19.9 MPa) and elongation at break (66.2–42.6%) of HIPS resins (Table IV) decreased along with T3 concentration increased, while displacement at break reduced from 13.5 to 8.5 mm (Figure 4).

HIPS-7 and HIPS-18 were attained by D2 and T3 initiator, respectively. With the same SIBR-2 content of 20% and initiator concentration of 0.1%, HIPS-7 presented higher impact strength (12.9 kJ/m^2) compared with HIPS-18 (6.5 kJ/m^2). This result was mainly due to the relatively enhanced RPVF parameter and higher M_w of HIPS-7 induced by D2.

Fracture Morphology of HIPS Resins

The details of fracture information were recorded by scanning electron microscopy (SEM) as shown in Figure 5. In order to concisely explain the micrograph of HIPS resins, the fracture surface was separated into three regions (I, II, and III) along with the arrow direction of hammer attaching toward notch. Region I represented the crack-initiation process, and regions II and III represented the crack-propagation process. In the impact fracture testing, the crack-initiation region (region I) exhibited a narrower zone comparing with crack-propagation region (region II and III).

Figure 5(a–d) presented SEM micrographs of the impact-fractured surface of HIPS-6 specimen with SIBR of 15%. The micrograph of region I [Figure 5(a)] of HIPS-6 exhibited less ductile feature. When the region I was observed at a higher magnification [Figure 5(d)], the cavitations formation were detected. The void coalescence established the crack initiation feature in the HIPS-6 matrix. As shown in Figure 5(b), the crack-propagation process generated the craze marks in the region II. The craze phenomenon was distributed as discrete feature with low regularity. The branched craze occurred in region III [Figure 5(c)] of HIPS-6 as the distance from the notch tip increased, owing to the intersection between the initial and latter cracks.

As illustrated in Figure 5(e–h), the impact-fractured surface of HIPS-8 specimen with SIBR of 25% was also studied. Due to the incremental content of toughened rubber, HIPS-8 displayed better ductile behavior than HIPS-6. In the region I [Figure 5(e)], the fracture surface was rough near the notch tip, and the craze with extensive dimension occurred instead of cavitations. The primary crack-propagation was represented in Figure 5(f), the craze induced in region II possessed the intensive and regular feature. Then the craze further improved in region III [Figure 5(g)] with irregular extension. In the higher magnification of region III of HIPS-8 [Figure 5(h)], the apparent shear deformation was identified, revealing better ductile mode than HIPS-6. This morphology was also consistent with the mechanical property examined in the impact test.

CONCLUSIONS

HIPS resins were attained with in situ bulk polymerization toughened by one-pot SIBR. Nd-based catalyst showed high activity toward conjugated dienes rather than St, affording St solution of random SIBR with high 1,4-selectivity and low St content. The mixture was straightforward subject to free radical polymerization with difunctional initiator (D2) and trifunctional initiator (T3). Compared with SIBR-1 and SIBR-3, SIBR-2 exhibited preferable toughening effect. Increasing the rubber fraction in HIPS resins was beneficial to enhance the impact strength while tensile strength decreased. Raising the initiator amount (T3) caused decrease of impact strength and tensile strength. SEM analysis demonstrated the fracture surface morphology of HIPS specimens with high content of SIBR presented ductile fracture behavior and shear deformation, revealing the incremental rubber matrix displayed synergistic toughening effect of crazing.

ACKNOWLEDGMENTS

This work was financially supported by The National Basic Research Program of China (973 program) for Grant No. 2015CB654700 (2015CB654701), The National Nature Science Foundation of China for project Nos. 21404019, 21034001, 21174021, and The China Postdoctoral Science Foundation of project No. 2014M550154.

REFERENCES

1. Echte, A.; Gausepohl, H.; Lütje, H. *Angew. Makromol. Chem.* **1980**, *90*, 95.

2. Echte, A.; Haaf, F.; Hambrecht, J. *Angew. Chem. Int. Ed.* **1981**, *20*, 344.
3. Alfarraj, A.; Nauman, E. B. *Polymer* **2004**, *45*, 8435.
4. Meira, G. R.; Luciani, C. V.; Estenoz, D. A. *Macromol. React. Eng.* **2007**, *1*, 25.
5. Tung, L. H.; Kirkby, L. L.; Lyons, C. E. U.S. Pat. 4,311,819 (**1982**).
6. Lätsch, S.; Fischer, W.; Gausepohl, H.; Warzelhan, V.; Schade, C. U.S. Pat. 6,303,721 B1 (**2001**).
7. Short, J. N.; Hanmer, R. S. U.S. Pat. 3,299,178 (**1967**).
8. Windisch, H.; Obrecht, W.; Michels, G.; Steinhauser, N. U.S. Pat. 6,310,151 B1 (**2001**).
9. Hattori, Y.; Kitagawa, Y. U.S. Pat. 5,096,970 (**1992**).
10. Windisch, H.; Obrecht, W.; Michels, G.; Steinhauser, N.; Schnieder, T. U.S. Pat. 2003/0,134,999 A1 (**2003**).
11. Kobayashi, E.; Kaita, S.; Aoshima, S.; Furukawa, J. *J. Polym. Sci. A Polym. Chem.* **1995**, *33*, 2175.
12. Jin, Y.; Wang, P.; Pei, F.; Cheng, G.; Cui, L.; Song, C. *Polymer* **1996**, *37*, 349.
13. Kobayashi, E.; Hayashi, N.; Aoshima, S.; Furukawa, J. *J. Polym. Sci. A: Polym. Chem.* **1998**, *36*, 241.
14. Zhang, Q.; Ni, X.; Shen, Z. *Polym. Int.* **2002**, *51*, 208.
15. Friebe, L.; Nuyken, O.; Obrecht, W. *Adv. Polym. Sci.* **2006**, *204*, 1.
16. Rovere, J.; Correa, C. A.; Grassi, V. G.; Pizzol, M. F. D. *J. Mater. Sci.* **2008**, *43*, 952.
17. Bucknall, C. B.; Davies, P.; Partridge, I. K. *J. Mater. Sci.* **1987**, *22*, 1341.
18. Fischer, M.; Hellmann, G. P. *Macromolecules* **1996**, *29*, 2498.
19. Leal, G. P.; Asua, J. M. *Polymer* **2009**, 68.
20. Trifonova, D.; Vasileva, S. *J. Mater. Sci.* **1992**, *27*, 3657.
21. Trifonova, D.; Vasileva, S. *J. Mater. Sci. Lett.* **1993**, *12*, 695.
22. Nordsiek, K. H. *Kautsch Gummi Kunstst* **1985**, *38*, 178.
23. Yang, J.; Wang, J.; Liu, Y. *China Synth. Resin Plast.* **2005**, *22*, 58.
24. Yang, J.; Wang, C. X.; Yu, Z. S.; Li, Y.; Yang, K. K.; Wang, Y. Z. *J. Appl. Polym. Sci.* **2011**, *121*, 2458.
25. Du, X. X.; Li, Y.; Li, Z. S.; Yu, Z. S.; Wang, S. M.; Zhang, C. Q.; Wang, Y. R. *China Synth. Rubber Ind.* **2010**, *33*, 276.
26. Serpooshan, V.; Zokaei, S.; Bagheri, R. *J. Appl. Polym. Sci.* **2007**, *104*, 1110.
27. Choi, J. H.; Ahn, K. H.; Kim, S. Y. *Polymer* **2000**, *41*, 5229.
28. Vilaplana, F.; Karlsson, S.; Ribes-Greus, A.; Schade, C.; Nestle, N. *Polymer* **2011**, *52*, 1410.
29. Xue, Z.; Liu, X.; Zhuang, Q.; Hu, K.; Han, Z. *Polym. Compos.* **2012**, *33*, 430.
30. Silva, P. S. R. C.; Tavares, M. I. B. *Mater. Res.* **2015**, *18*, 191.
31. Li, T.; Hu, Y.; Zhang, X.; Shi, Z.; He, G.; Wang, Y.; Shen, K.; Li, Y. *J. Appl. Polym. Sci.* **2013**, *130*, 1772.
32. Xu, Q.; Li, L.; Guo, F.; Shi, Z.; Ma, H.; Wang, Y.; Wang, Y.; Li, Y. *Polym. Eng. Sci.* **2014**, *54*, 1858.
33. Xu, X.; Yang, H.; Zhang, H. *Eur. Polym. J.* **2005**, *41*, 1919.
34. Yu, Z.; Li, Y.; Zhao, Z.; Zhang, C.; Yang, J.; Zhang, C.; Li, Z.; Wang, Y. *Polym. Eng. Sci.* **2009**, *49*, 2249.
35. Yu, Z.; Li, Y.; Wang, Y.; Li, Y.; Liu, Y.; Li, Y.; Li, Z.; Zhao, Z. *Polym. Eng. Sci.* **2010**, *50*, 961.
36. Feng, H.; Zhang, X.; Zhao, S. *J. Appl. Polym. Sci.* **2008**, *110*, 228.
37. Liu, D.; Cui, D. *Dalton Trans.* **2011**, *40*, 7755.
38. Wang, Z.; Wang, Y.; Li, Y.; Xu, H.; Ren, Y.; Zhang, C. *J. Appl. Polym. Sci.* **2006**, *102*, 5848.
39. Canavate, J.; Pages, P.; Saurian, J.; Colom, X.; Carrasco, F. *Polym. Bull.* **2000**, *44*, 293.